REGIONALLY APPLICABLE ANGULAR REFLECTANCE MODELS

J. M. Davis
Colorado State University
Fort Collins, Colorado

INTRODUCTION

The inference of the reflected component of the Earth's radiation budget from medium- or narrow-field-of-view radiometer measurements requires knowledge of the angular variation of the reflected radiance field. Arking (1965), Ruff et al. (1968), Salomonson and Marlatt (1968), Salomonson (1968), Griggs and Margraff (1967), Bartman (1968), and Brennan and Bandeen (1970) have investigated the angular variation of upwelling radiance fields, and in general they have found a significant degree of anisotropy in almost every type of reflecting surface with the possible exception of desert sand. One of the major tasks of the Earth Radiation Budget Experiment (ERBE) is to compile a data base which could be used to produce adequate angular reflectance models. Updates on this effort may be found in Stowe et al. (1980) and Stowe and Taylor (1981). Minnis and Harrison (1980) have used bidirectional reflectance models in developing a methodology for estimating cloud parameters from geostationary satellite data.

MODEL DESCRIPTION

The present research is similar to the works cited above in that one of the major goals is to establish the nature of the angular variation of reflected radiance fields. However, the present research attempts to define the average angular model over a spatial scale pertinent to regional climate modeling or monitoring, i.e., from 250 to 1000 km. Important information is also provided regarding the nature of the convergence of the radiance patterns to the regional means. This research is based on data collected during Summer Monex 1979 using a multidetector instrument described by Davis et al. (1982). (See fig. 1.) The instrument was flown on NASA's Convair 990 research aircraft at altitudes above 30 000 feet over a variety of surfaces, from the broken ice fields of Hudson Bay to the desert sands of the Saudi Arabian Peninsula. The radiances measured over the scenes were averaged and then normalized by multiplying by π and dividing by the scene-averaged reflected flux density. This cast the models into the inverse of the bidirectional reflectance normalization coefficient, which has a value of unity for an isotropic surface.

When this quantity was compared with the same quantity derived from many of the works cited previously, agreement was generally good (≃10 percent rms) except in two cases, the 70° to 80° solar zenith angle desert case (compared to a model based on Salomonson's (1968) data) and a 40° to 50° ocean model (compared to a model generated from the data of Brennan and Bandeen (1970)). Comparison of these cases with the data of Salomonson and Brennan and Bandeen resulted in an rms difference of 0.43 and 0.21, respectively, between normalized radiances evaluated at 105 points in a nadir-relative azimuth angle coordinate system.

(See figs. 2 and 3.) In the first case the discrepancies were most likely the result of the forward scattering of the dust-laden atmosphere prevalent during Summer Monex. Salomonson's data were collected at relatively low altitudes (approximately 300 m), limiting the atmospheric contribution. In the second case the differences result primarily from the lack of a Sun glint feature in the data of Brennan and Bandeen, which may have resulted from a rough sea state. Nevertheless, it is obvious that significantly different values of reflected flux density would be inferred depending upon which data are utilized in these cases.

The multidetector design of the data collection instrument allowed for the sampling of the upwelling radiance field from 12 directions simultaneously. These data may be analyzed to reveal the nature of the spatial convergence of the radiances to the regional models. If bidirectional reflectance models are used to infer the reflected flux density of a region, it is important to insure that the model is representative of the region. Spatial variations in the radiance fields should be considered as carefully as angular variations in this regard.

For example, consider the following numerical experiment. Let us assume that the reflected flux density E_i at a point i is given by

$$E_i = k \sum_{j=1}^{12} n_{ij} \cos \theta_j \, \Delta\omega_j$$

where

n_{ij} radiance measurement at the ith point from the jth sensor

θ_j nadir angle of the jth sensor

$\Delta\omega_j$ solid angle subtended by the field of view of the jth detector

k factor which scales E, the scene average of reflected flux density E_i, to E', the scene average of the reflected flux density E_i' as measured by an Eppley pyranometer. (Actually, E_i and E_i' differ by about 10 percent rms over a particular scene.)

If, for a particular scene, we use the set of measurements n_{ij} and the scene average of E_i to form a bidirectional reflectance model, we may then examine the convergence of the inferred to the actual value of E as a function of averaging distance and the number of measurements or satellites. Table 1 shows the results of such an analysis for the 10° to 20° clear ocean data. The entries in the table represent the percentage difference between the average of E_i over the given distance and the average of the inferences of the same quantity using the appropriate bidirectional reflectance model. Also, the results represent averages with respect to which sensor or combination of sensors was used to make the inference. For example, if n sensors were used to make an inference, the table entry is an average over all of the possible $C\binom{12}{n}$ sensor combinations.

The results in table 1 may be interpreted as follows. An inference of the flux density reflected from the ocean for solar zenith angles between 10° and 20° may be made to within 6 percent accuracy along a 50-km path if the averages from 12 angular positions are taken, or to about the same accuracy if the scene is viewed from two angular coordinates for a distance of 200 km. Similar analyses of other atmospheric scene types indicate that the so-called "clear" ocean scene with its attendant fair-weather cumulus distributions requires the greatest effort from both the angular and the spatial sampling standpoints in order to obtain a meaningful flux density inference.

CONCLUSION

The results of this study support the premise that the reflected component of the Earth's radiative budget may be inferred to an accuracy of about 2.5 percent with medium- or narrow-field-of-view radiometers if (1) the appropriate regionally averaged bidirectional reflectance models are used, (2) adequate spatial sampling is maintained (generally greater than 200 km and less than 1000 km), and (3) the inference is derived from adequate angular sampling (from one to four angular viewing coordinates).

REFERENCES

Arking, A. 1965: The Angular Distribution of Scattered Radiation and the Earth Albedo as Observed From TIROS. Goddard Institute for Space Studies, Annual Res. Rept., June, pp. 47-67.

Bartman, F. L. 1968: Earth Reflectance Patterns Measured by Radiometer on High Altitude Balloon Flights. Tech. Rept. 05863-13-T, Univ. of Michigan (Contract NASr-54(03)), 15 pp.

Brennan, B.; and Bandeen, W. R. 1970: Anisotropic Reflectance Characteristics of Natural Earth Surfaces. Appl. Opt., vol. 9, no. 2, pp. 405-412.

Davis, J. M.; and Cox, S. K. 1980: Radiance Patterns Over Extended Regions. Proceedings of the International Radiation Symposium, American Meteorological Society, Boston, pp. 370-327.

Griggs, M.; and Margraff, W. A. 1967: Measurement of Cloud Reflectance Properties and the Atmospheric Attenuation of Solar and Infrared Energy. Report prepared by the General Dynamics Corporation, Convair Division, San Diego, Ca. (Contract AF19(628)-5517), 153 pp.

Minnis, P.; and Harrison, E. F. 1980: A Methodology for Estimating Cloud Parameters From Geostationary Satellite Infrared and Visible Data. Proceedings of the International Radiation Symposium, American Meteorological Society, Boston, pp. 340-342.

Ruff, I.; Koffler, R.; Fritz, S.; Winston, J. S.; and Rao, P. K. 1968: Angular Distribution of Solar Radiation Reflected From Clouds as Determined From TIROS IV Radiometer Measurements. J. Atmos. Sci., vol. 25, no. 2, pp. 323-332.

Salomonson, V. V.; and Marlatt, W. E. 1968: Anisotropic Solar Reflectance Over White Sand, Snow, and Stratus Clouds. Atmos. Sci. Paper No. 120, Colorado State Univ., Ft. Collins, 41 pp.

Salomonson, V. V. 1968: Anisotropy in Reflected Solar Radiation. Atmos. Sci. Paper No. 128, Colorado State Univ., Ft. Collins, 142 pp.

Stowe, L. L.; Jacobwitz, H.; and Taylor, V. R. 1980: Reflectance Characteristics of Earth and Cloud Surfaces as Measured by the ERB Scanning Channels on the Nimbus 7 Satellite. Proceedings of the International Radiation Symposium, American Meteorological Society, Boston, pp. 430-432.

Stowe, L. L.; and Taylor, V. P. 1981: Emission Characteristics of Earth and Cloud Surfaces as Measured by the ERB Scanning Channels on the Nimbus 7 Satellite. Proc. Fourth Conference on Atmospheric Radiation, American Meteorological Society, Boston, pp. 124-127.

TABLE 1.- PERCENTAGE ERROR IN INFERENCE OF REFLECTED FLUX DENSITY AS A FUNCTION OF AVERAGING DISTANCE AND NUMBER OF ANGULAR SAMPLING COORDINATES

[10° to 20° clear ocean scene]

Averaging distance, km	Error, percent, when number of measurements (satellites) is -											
	1	2	3	4	5	6	7	8	9	10	11	12
1	32.9	23.5	19.3	16.9	15.2	14.0	13.1	12.3	11.7	11.2	10.7	10.4
2	32.3	23.0	19.0	16.6	14.9	13.7	12.8	12.1	11.5	11.0	10.5	10.2
10	26.5	19.0	15.8	13.9	12.6	11.7	11.0	10.5	10.0	9.6	9.3	9.0
20	22.1	15.8	13.1	11.5	10.4	9.6	9.0	8.5	8.1	7.8	7.5	7.3
50	16.6	12.0	10.1	9.0	8.2	7.7	7.2	6.9	6.7	6.4	6.3	6.1
100	12.0	8.7	7.4	6.6	6.0	5.7	5.4	5.2	5.0	4.8	4.7	4.6
200	8.4	6.3	5.4	4.9	4.6	4.4	4.2	4.1	4.0	3.9	3.9	3.8

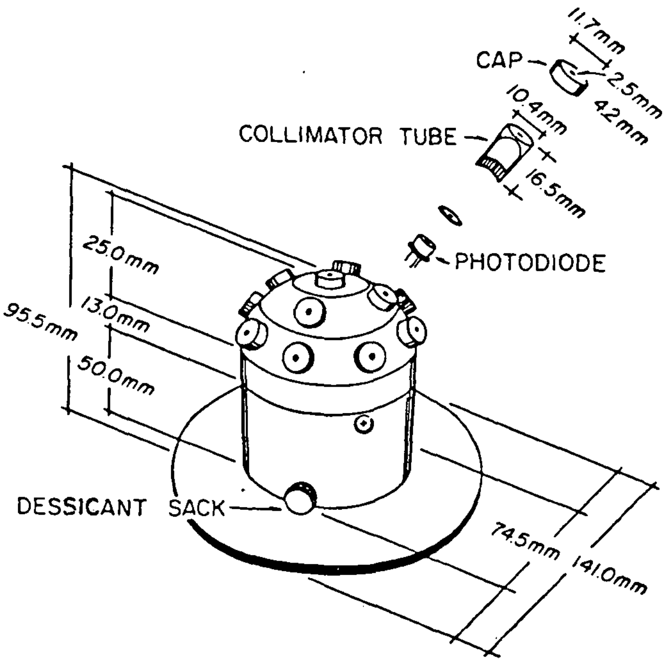

Figure 1.- Schematic of the multidetector instrument used for measuring reflected radiances.

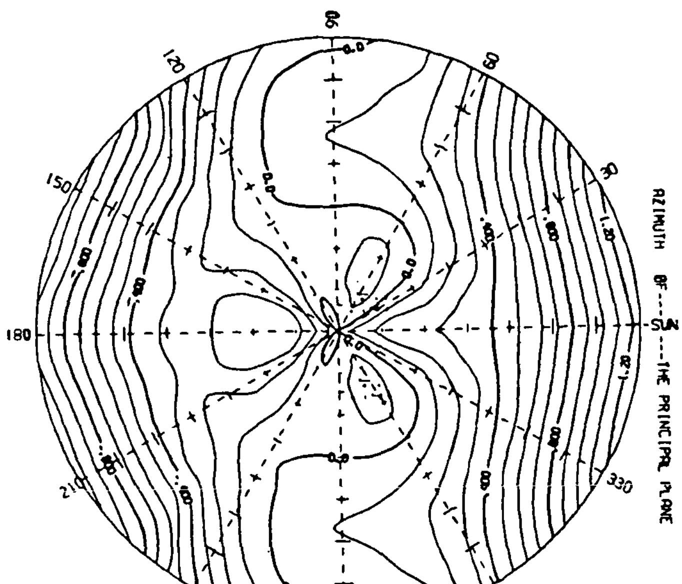

Figure 2.- Contours of differences between normalized reflected radiances from the present study and the same quantity from data of Salomonson (1968) for a 70° to 80° solar zenith angle desert scene. Positive values indicate that brighter features were measured in the present study. Contours are plotted as a function of observation nadir (increasing from 0° at the center to 70° at the rim) and azimuth measured relative to the solar azimuth.

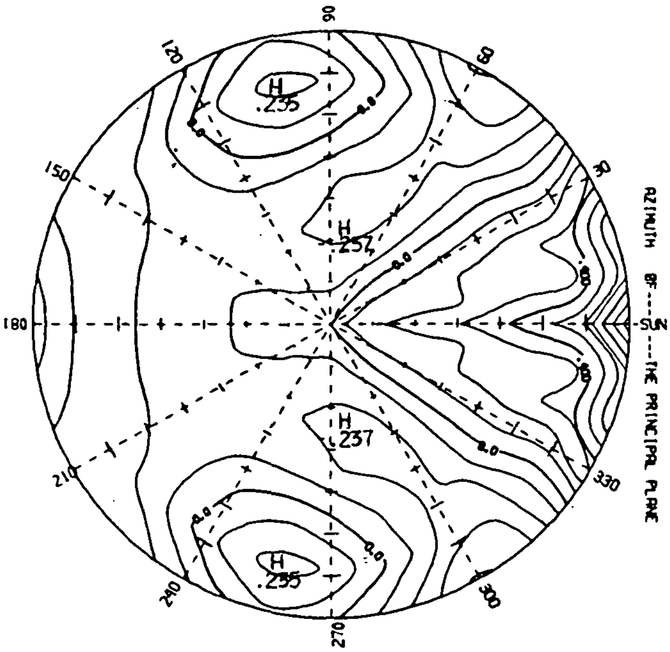

Figure 3.- Contours of differences between normalized reflected radiances from the present study and the same quantity from data of Brennan and Bandeen (1970) for a 40° to 50° solar zenith angle ocean scene. Positive values indicate that brighter features were measured in the present study. Contours are plotted as a function of observation nadir (increasing from 0° at the center to 70° at the rim) and azimuth measured relative to the solar azimuth.